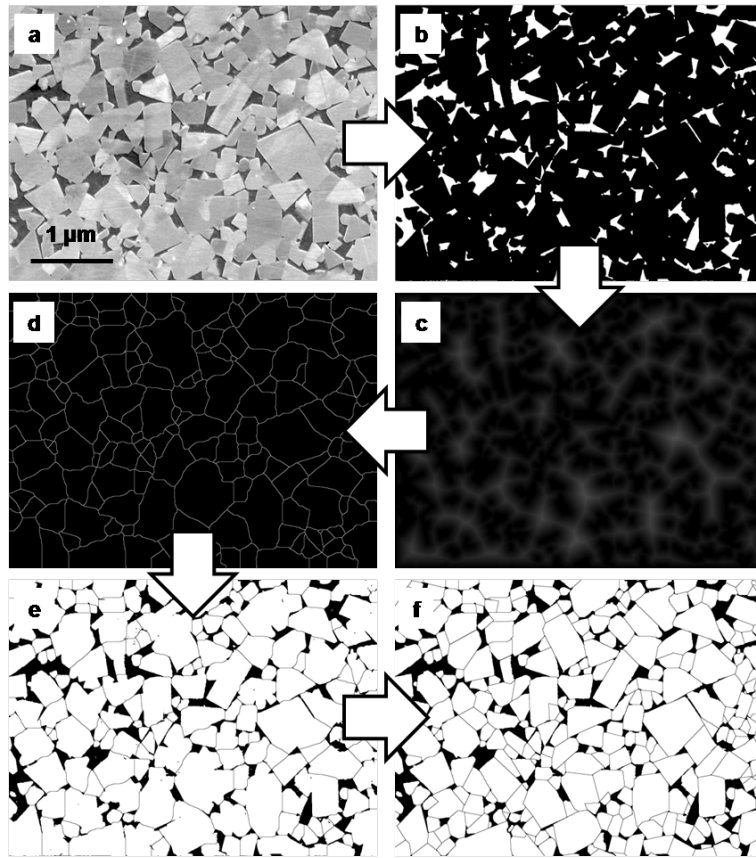


<b>Nomenclature</b>	<b>Binder content (%<sub>wt.</sub>)</b>	<b>Grain size</b>
6UF	6	Ultrafine
10UF	10	Ultrafine
15UF	15	Ultrafine
9F	9	Fine
11M	11	Medium
15M	15	Medium
10C	10	Coarse

**Table 1.** Nomenclature, binder content and grain size of investigated cemented carbides grades.



**Figure 1.** Schematic representation of the image processing methodology used to assess the grain size of investigated materials. Presented micrographs correspond to: (a) the initial FESEM micrograph, (b) the binarization of the original image followed by (c) a EDM algorithm, (d) a Find Maxima operation and (e) a OR operation between the binarized original image (Figure 1d) and the micrograph resulting from the Find Maxima operation (Figure 1d), and (f) the final processed and manually corrected image.

<b>Nomenclature</b>	<b>LI</b> <b><math>d_{WC}</math> (<math>\mu\text{m}</math>)</b>	<b>IA – A</b> <b><math>d_{WC}</math> (<math>\mu\text{m}</math>)</b>	<b>IA – B</b> <b><math>d_{WC}</math> (<math>\mu\text{m}</math>)</b>	<b>IA – A</b> <b>Circularity</b>
6UF	$0.4 \pm 0.21$	$0.39 \pm 0.22$	$0.56 \pm 0.25$	$0.69 \pm 0.07$
10UF	$0.39 \pm 0.19$	$0.42 \pm 0.20$	$0.49 \pm 0.21$	$0.67 \pm 0.11$
15UF	$0.47 \pm 0.22$	$0.46 \pm 0.24$	$0.55 \pm 0.27$	$0.68 \pm 0.10$
9F	$0.77 \pm 0.78$	$0.78 \pm 0.47$	$0.97 \pm 0.62$	$0.70 \pm 0.11$
11M	$1.12 \pm 0.71$	$1.29 \pm 0.58$	$1.55 \pm 0.76$	$0.70 \pm 0.12$
15M	$1.15 \pm 0.92$	$1.08 \pm 0.59$	$1.29 \pm 0.71$	$0.71 \pm 0.08$
10C	$2.45 \pm 1.37$	$2.39 \pm 1.15$	$2.67 \pm 1.40$	$0.72 \pm 0.11$

**Table 2.** Average grain size determined for investigated cemented carbides grades following the linear intercept and image analysis methods. Information on the circularity values obtained with the IA – A process is also included.

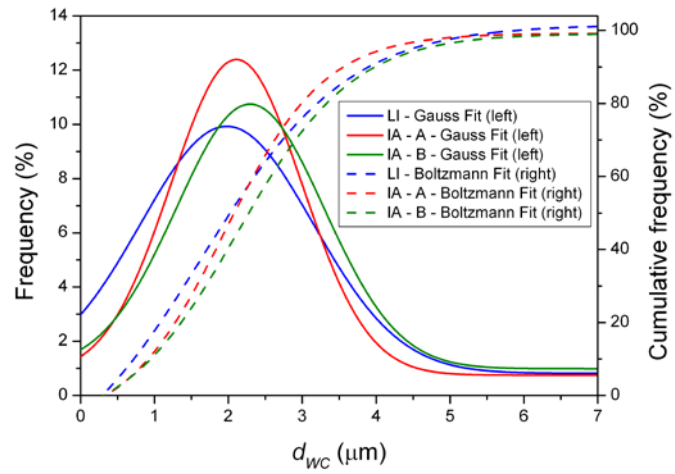


**Figure 2.** Comparison of the relative and cumulative distributions determined following the linear interception and image analysis studied methods for the investigated 11M hardmetal grade.

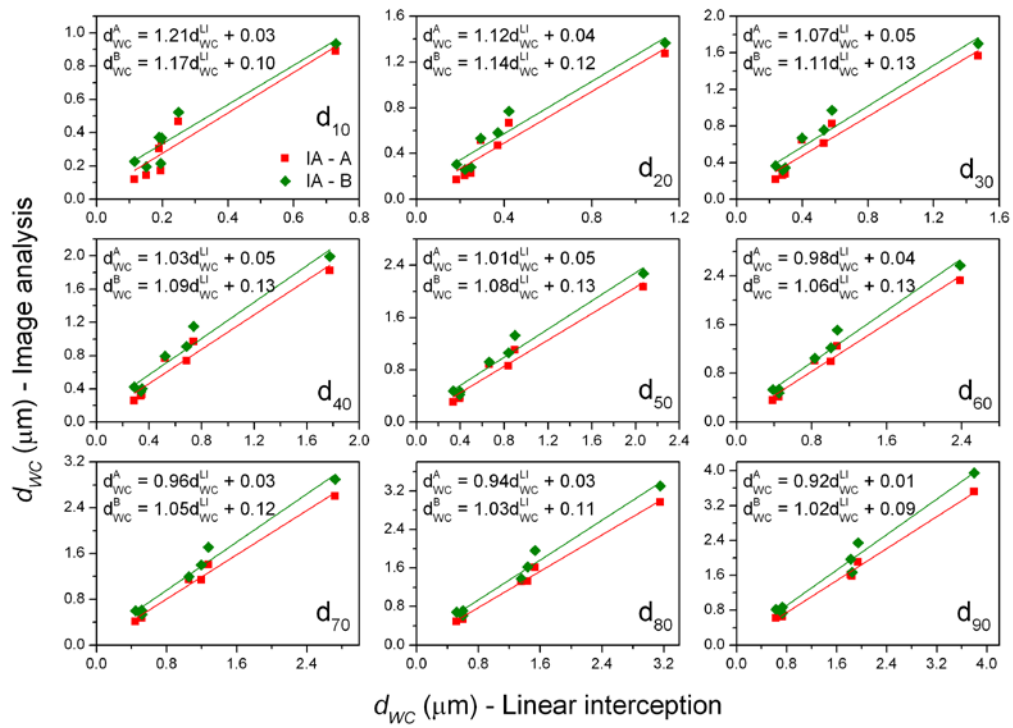


**Figure 3.** Comparison between grain size values deduced from the cumulative distributions corresponding to the linear interception and image analysis techniques for different cumulative distribution percentages.

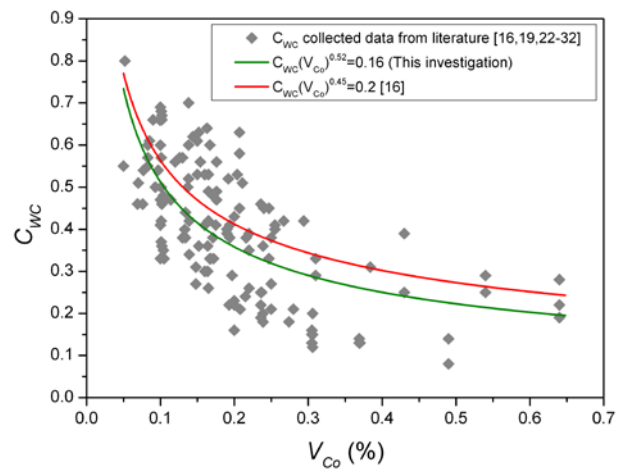


**Figure 4.** Contiguity dependence on the binder volume content (data collection from literature [17,20,23–33]). Full lines correspond to the best fitting curves proposed in pervious works (red line) [1,17] and in this investigation (green line).

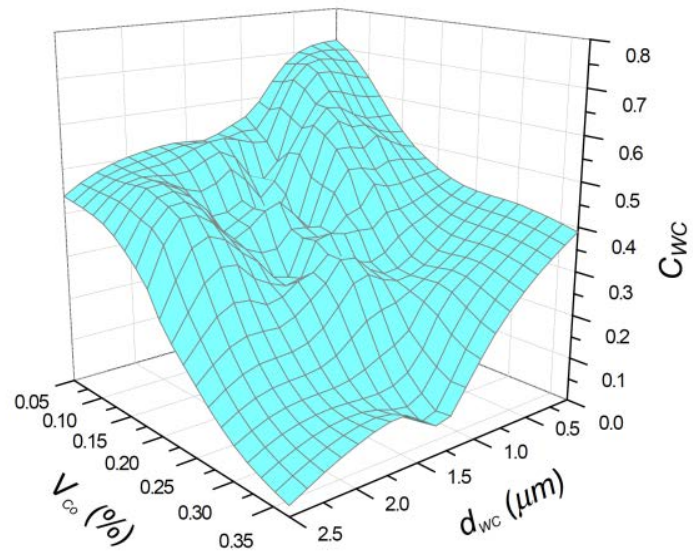


**Figure 5.**  $C_{WC}$  values plotted as a function of mean grain size and of the binder volume content  $V_{binder}$ , as independent variables.

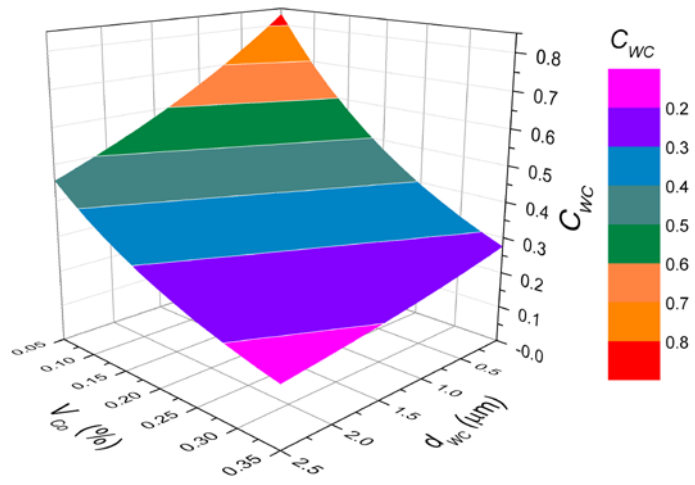


**Figure 6.**  $C_{WC}$  values plotted as a function of  $d_{WC}$  and  $V_{binders}$  as independent variables according to best fitting parameters determined for Eq. (4).



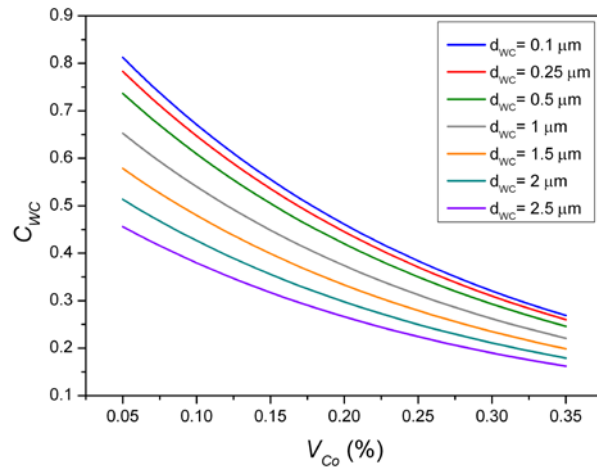


**Figure 7.** Contiguity as a function of the binder content for different mean grain size levels.

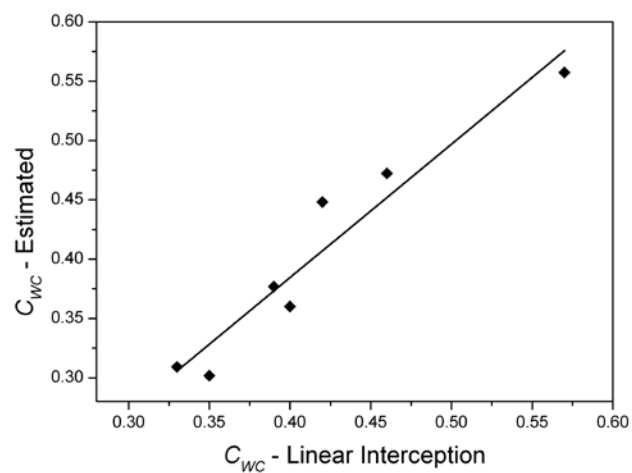


**Figure 8.** Linear dependence between the contiguity values experimentally determined following the linear interception technique and the values estimated according to the empirical proposed in Eq. (4).